

## Reflection and transmission of a wave incident on a slab with a time-periodic dielectric function $\epsilon(t)$

Jorge R. Zurita-Sánchez, P. Halevi, and Juan C. Cervantes-González

*Instituto Nacional de Astrofísica, Óptica y Electrónica, Apartado Postal 51, Puebla, Pue. 72000, Mexico*

(Received 16 January 2009; published 12 May 2009)

We present a theoretical description of the response of a dynamic slab, with time-periodic dielectric function  $\epsilon(t)$ , to a normally incident monochromatic plane wave of frequency  $\omega_o$ . As a consequence of the interaction of this incoming wave with the dynamic slab, the reflected and transmitted waves contain harmonics of the modulating frequency  $\Omega$ , namely, the slab itself becomes a polychromatic source of frequencies  $\omega_o - n\Omega$  ( $n = 0, \pm 1, \pm 2, \dots$ ). We establish a general formalism to quantify the reflected and transmitted fields for any periodic variation in the dielectric function. To achieve this, a description of wave propagation in a dynamic bulk is needed. A theoretical framework to treat such propagation, based on the concept of a *temporal photonic crystal*, is developed. As a consequence of the Bloch-Floquet theorem, the dispersion relation is a band structure that is periodic with frequency and exhibits forbidden *wave vector* gaps. The Poynting vectors of the transmitted and reflected fields are analyzed in detail. Our theory is applied to the case in which the dielectric function is modulated sinusoidally. We calculate numerically the magnitudes and phases of the reflection and transmission coefficients for several harmonics  $\omega_o - n\Omega$  and slab thicknesses. Three modulation regimes are considered: weak, moderate, and strong. The response in the weak regime is similar to that of a Fabry-Perot etalon—the strengths of the harmonics are weak. For the strong-modulation regime, the strengths of reflection and transmission coefficients of the harmonics become large; they can even exceed one due to the openness of the system in which an external modulating agent can provide part of the invested energy. Dynamic variation in the dielectric properties of materials can give rise to new effects in wave propagation and to novel optical applications and is readily attainable with present-day technology.

DOI: [10.1103/PhysRevA.79.053821](https://doi.org/10.1103/PhysRevA.79.053821)

PACS number(s): 42.25.Bs

### I. INTRODUCTION

This paper concerns electromagnetic wave propagation in a *dynamic or active* medium, namely, the dielectric function  $\epsilon(t)$  that characterizes the medium is time dependent. While such temporal inhomogeneity has been studied much less than its spatial counterpart  $\epsilon(\mathbf{r})$ , dynamic media arose interest for many decades. Engineering applications of signal manipulation, with applications such as modulators, parametric amplifiers, and frequency converters, were contemplated half a century ago [1,2]. These pioneering publications and some that followed assumed the existence of a pump wave modulating the medium both in space and in time [3].

Dynamic behavior can also result from a powerful electromagnetic pulse that ionizes a plasma. Such an experiment, first performed by Yablonovitch [4], caused an abrupt modification of the dielectric function and upshifting of the frequency of the incident wave. It was also suggested by Yablonovitch [5] that the sudden creation of electron-hole pairs in a semiconductor by photoexcitation could reduce the dielectric constant from  $\sim 12$  to 0 in a brief time period. *A propos*, Juršenas *et al.* [6] have recently experimented with high photoexcitation in GaN; as a result of electron-hole recombination, the initial free-electron density decayed from  $\sim 10^{19}$  to  $3 \times 10^{18}$   $\text{cm}^{-3}$  in a time about 800 ps. Clearly, this gives rise to a notable variation in the dielectric constant. In this category of nonstationary interfaces, we also mention the application of a shock wave to a photonic crystal, resulting in dramatic changes in its optical properties within an extremely short time interval [7,8]. Finally a different approach to moving interfaces was taken by Biancalana *et al.* [9], who

studied the dynamics of light propagation in media possessing an arbitrary layered space-time dependence of the refractive index, leading to effects such as pulse shaping.

A more rigorously controllable modulation in time of the dielectric constant is based on nonlinear behavior, such as the electro-optic and thermo-optics effects. In this active line of research, Park and Summers [10] reported extraordinary diffraction and dispersion in two-dimensional photonic crystal slabs. Also, Scrymgeour *et al.* [11] showed how to tune the superprism effect. Yanik *et al.* [12–14] simulated pulse propagation in photonic crystal waveguides coupled to resonators that are assumed to be tuned in real time, electro-optically, or nonlinearly. By taking advantage of the thermo-optic effect, Vlasov *et al.* [15] were able to actively control slow light on a chip with a photonic crystal waveguide. Further, Notomi and Mitsugi [16] simulated wavelength conversion of light by means of dynamical tuning of the refractive index.

We single out a particularly promising method of active electro-optic tuning based on the *plasma dispersion effect* [17–21]. Here the density of free electrons and/or holes in a semiconducting component is modulated in real time by means of a voltage or pumping, or temperature, etc. As a consequence, the dielectric constant of the semiconductor becomes time dependent and the entire system becomes active. However, the typical changes in the dielectric constant are very small ( $\sim 10^{-3}$ ). It was, nevertheless, demonstrated by Barrios *et al.* [22] that this limitation can be overcome by the use of a highly confined *resonant* structure, namely, silicon microring resonators. Exploiting this concept, Lipson and co-workers [23,24] led to characteristic modulation and switching times of less than 1 ns.

While modulation at optical frequencies would be difficult at present, it should be noted that electro-optic modulators for harmonic generation are actually commercially available. The modulation in these devices is generated by microwave fields ( $\sim 1$  GHz) of wavelength that is much larger than the slab's thickness. Consequently, the modulation can be considered to be purely temporal to a good approximation. Note, however, that no detailed and exact theory, describing this behavior, is available to our knowledge. While the typical strength of an electro-optic modulator is very small  $\Delta\epsilon/\epsilon \sim 10^{-4}$ , strong modulation can be achieved in ferroelectrics in the microwave regime ( $\Delta\epsilon/\epsilon \lesssim 1$ ) using sufficiently strong applied fields. In fact, such modulation at GHz frequencies is now being planned in the Microwave Laboratory of our institute.

Finally, we note that a convenient manner of tuning the band structure of photonic crystals is by means of liquid crystal infiltration, given the fact that the nematic molecules of a liquid crystal are highly manipulable by an external electric or magnetic field, temperature, etc. [25–27].

An important subclass of dynamic media, with the dielectric function varying *periodically* in time (however independent of the position), is our subject in this paper. Particular cases of  $\epsilon(t)$  were studied before: harmonic variation (in the long-wavelength limit of the pump wave) [1,3], a special variation chosen to lead to Mathieu functions for the eigenfunctions [2], and rectangular (Kronig-Penney type) [9]. The last-mentioned, very recent, paper by Biancalana *et al.* [9] actually treats the rectangular profile as one application of a theory of “spatiotemporal” dielectric structures. Our intention here is to present an in-depth study of electromagnetic wave propagation in the bulk and for a slab, assuming that  $\epsilon(t)$  is an *arbitrary periodic function*. We will establish the general properties of the eigenvalues (band structure) and eigenfunctions for the electric field. Also, the instantaneous Poynting vector will be treated. Further, we will calculate the electric fields that are reflected and transmitted when a plane wave is incident on a slab characterized by an  $\epsilon(t)$  of arbitrary periodicity. We will establish that the reflected and transmitted fields are composed of all harmonics produced by the periodic modulation. As for the fields within the slab, in addition to the same harmonics, they are also superpositions of waves with different values of the wave vector, corresponding to permitted *wave vector bands*. These analytic conclusions will be corroborated by numerical calculations.

A dielectric medium characterized by a periodically varying dielectric function  $\epsilon(t)$  may be considered as a *temporal photonic crystal*. Not surprisingly, such a medium does *not* exhibit *frequency gaps*, well known to occur in case of *spatial* periodicity of the medium, namely, for (ordinary) photonic crystals. For temporal periodicity of  $\epsilon(t)$ , *wave vector* or *k gaps* are created, as already realized before [2,9]. We will show, in fact, that propagation is possible only if  $k(=|\mathbf{k}|)$  lies inside a permitted *k band*. It is worthwhile mentioning that *k gaps* (or momentum gaps) can also arise from other origins: periodic modulation of the gain in a waveguide [28,29] and surface plasmons propagating on corrugated metallic surfaces [30–34].

For the sake of generality, we will not concern ourselves with the origin of the temporal variation, considering this to

be extraneous to the problem at hand. Nevertheless, in order to give the reader some intuition in this regard, let us take a look at the very simple case of a small harmonic variation,

$$\epsilon(t) = \epsilon_0[1 + \kappa \sin(\Omega t)], \quad \kappa \ll 1. \quad (1)$$

This may be viewed as parametric modulation of the dielectric function, realized, for example, optically or acoustically. Now considering—admittedly *naively*—that the electric field is a plane harmonic wave, the displacement vector is

$$\begin{aligned} \mathbf{D}(\mathbf{r}, t) &= \epsilon_o \epsilon(t) \mathbf{E}_o e^{i(\mathbf{k}\cdot\mathbf{r} - \omega t)} = \epsilon_o \epsilon_0 \mathbf{E}_o e^{i(\mathbf{k}\cdot\mathbf{r} - \omega t)} \\ &+ \epsilon_o \epsilon_0 [\mathbf{E}_o e^{i(\mathbf{k}\cdot\mathbf{r} - \omega t)}] [\kappa \sin(\Omega t)]. \end{aligned} \quad (2)$$

The second term can be interpreted as arising from the interaction of the plane wave of frequency  $\omega$  with a *long-wavelength* wave of frequency  $\Omega$ . This may be compared with the coupled-wave theory although the stress there is on spatial modulation, whereas this paper deals with temporal modulation. Because  $\kappa \ll 1$ , the pump wave can be considered to give rise to a weak nonlinearity. An instructive way to rewrite the last equation is

$$\begin{aligned} \mathbf{D}(\mathbf{r}, t) &= \epsilon_o \epsilon_0 \mathbf{E}_o e^{i(\mathbf{k}\cdot\mathbf{r} - \omega t)} + \frac{\epsilon_o \epsilon_0 \kappa}{2} \mathbf{E}_o e^{i[\mathbf{k}\cdot\mathbf{r} - (\omega + \Omega)t + \pi/2]} \\ &+ \frac{\epsilon_o \epsilon_0 \kappa}{2} \mathbf{E}_o e^{i[\mathbf{k}\cdot\mathbf{r} - (\omega - \Omega)t - \pi/2]}. \end{aligned} \quad (3)$$

The interaction between the two waves thus produces two secondary or satellite plane waves. These have small amplitudes  $\sim \kappa \mathbf{E}_o$  and frequencies  $\omega \pm \Omega$ . This describes sum and difference frequency mixing. Thus, because  $\kappa \ll 1$ , this situation may be considered to correspond to weak nonlinearity. However, let us stress that such nonlinearity exists only if connection is made to *the excitation problem* as, in our example, the modulation of frequency  $\Omega$ . Indeed, the treatment in the following sections is strictly linear.

This paper is organized as follows. In Sec. II, we present the theory of wave propagation in a time-periodic bulk medium. This section begins with the Maxwell equations without imposing any restriction (other than isotropy) on the dielectric function. Then, after limiting ourselves to only time-periodic dielectric functions, the general eigenvalue problem is solved, that is, the general properties of the dispersion relation (band structure) and of the electric field eigenfunctions are investigated. The section ends by presenting the density of modes in the medium. Section III is dedicated to the theory of the reflection and transmission of a plane wave incident normally at a time-periodic dynamic slab. In the same section, the Poynting vectors of the reflected and transmitted fields from the slab are analyzed. In Sec. IV, we apply the theory to simulate numerically particular cases of harmonic variation in  $\epsilon(t)$ . The paper is wrapped up in Sec. V. Finally, Appendixes A–D supplement and treat certain specific calculations.

## II. WAVE PROPAGATION IN A BULK DYNAMIC MEDIUM

### A. Wave equation

We consider a bulk, uniform, nonmagnetic, isotropic, non-dispersive, and nonabsorbing medium with a time-dependent dielectric constant  $\epsilon(t)$ . We assume that free charges are absent, thus the current density  $\mathbf{J}$  and the charge density  $\rho$  vanish. Then, the Maxwell equations in mks units are

$$\nabla \cdot \mathbf{E} = 0, \quad (4a)$$

$$\nabla \cdot \mathbf{H} = 0, \quad (4b)$$

$$\nabla \times \mathbf{E} = -\mu_o \frac{\partial \mathbf{H}}{\partial t}, \quad (4c)$$

$$\nabla \times \mathbf{H} = \frac{\partial}{\partial t} [\epsilon_o \epsilon(t) \mathbf{E}]. \quad (4d)$$

Here,  $\mathbf{E}(\mathbf{H})$  is the electric (magnetic) field and  $\epsilon_o$  are  $\mu_o$  are the vacuum electric permittivity and magnetic permeability, respectively. Since the medium is nonmagnetic, the constitutive relation for the magnetic induction field is  $\mathbf{B} = \mu_o \mathbf{H}$ . On the other hand, the constitutive relation for the displacement field is  $\mathbf{D} = \epsilon_o \epsilon(t) \mathbf{E}$ . The Maxwell equations [Eq. (4)] can be manipulated to yield the following wave equations for the electric  $\mathbf{E}$  and magnetic  $\mathbf{H}$  fields:

$$\nabla^2 \mathbf{E} - \frac{1}{c^2} \frac{\partial^2}{\partial t^2} [\epsilon(t) \mathbf{E}] = 0, \quad (5)$$

$$\nabla^2 \mathbf{H} - \frac{1}{c^2} \frac{\partial}{\partial t} \left[ \epsilon(t) \frac{\partial \mathbf{H}}{\partial t} \right] = 0, \quad (6)$$

$c$  being the speed of light in vacuum.

For completeness and future use, we derive the continuity conditions for an abrupt steplike change in  $\epsilon(t)$  at a certain time  $t_o$  in Appendix A.

### B. Dispersion relation and modes

Hereafter, we restrict ourselves to the case in which the dielectric constant is periodic in time, namely,

$$\epsilon(t) = \epsilon(t + T), \quad (7)$$

where  $T$  is the period. Equation (5) has plane wave solutions of the form

$$E(y, t) = E(t) e^{iky}, \quad (8)$$

where  $k$  is an arbitrary wave vector. Here, without loss of generality, we assume that the plane wave propagates in the  $y$  direction. Since the electric field is transverse [see Eq. (4a)], it must then lie in the  $zx$  plane. Substituting Eq. (8) into Eq. (5), we find that  $E(t)$  fulfills the equation

$$\frac{d^2}{dt^2} [\epsilon(t) E(t)] + k^2 c^2 E(t) = 0. \quad (9)$$

This wave equation is solved by means of the Bloch-Floquet theorem, implying that

$$E(t) = \bar{E}(\omega, t) e^{-i\omega t}, \quad (10)$$

where  $\bar{E}(\omega, t)$  is periodic in time with the period  $T$  and  $\omega$  is the characteristic *Bloch angular frequency*. Now, we aim to determine the dispersion relation  $\omega(k)$  and the electromagnetic modes. Since the dielectric constant varies periodically, we can expand it in a Fourier series as

$$\epsilon(t) = \sum_n \epsilon_n e^{in\Omega t}, \quad (11)$$

where  $\Omega \equiv 2\pi/T$  and  $n$  runs over all integers. Similarly,  $\bar{E}(\omega, t)$  admits a Fourier series representation, thus

$$\bar{E}(\omega, t) = \sum_n e_n(\omega) e^{in\Omega t}. \quad (12)$$

By using Fourier expansions (11) and (12) in Eq. (9), we obtain

$$\sum_n [\gamma_m(\omega) \epsilon_{m-n} - k^2 c^2 \delta_{mn}] e_n(\omega) = 0, \quad (13)$$

$$m, n = 0, \pm 1, \pm 2, \dots,$$

where  $\delta_{mn}$  is the Kronecker-delta tensor and

$$\gamma_m(\omega) \equiv (\omega - \Omega m)^2. \quad (14)$$

Equation (13) is a set of linear equations that connects the amplitudes  $e_n$  of all partial waves for all  $n$ . This set of equations defines an eigenvalue problem and has a nontrivial solution if the determinant of the amplitude coefficients vanishes. This is explicitly written as

$$\begin{vmatrix} \dots & \dots & \dots & \dots & \dots \\ \dots & \alpha_{-1} & \epsilon_{-1} \gamma_{-1} & \epsilon_{-2} \gamma_{-1} & \dots \\ \dots & \epsilon_1 \gamma_0 & \alpha_0 & \epsilon_{-1} \gamma_0 & \dots \\ \dots & \epsilon_2 \gamma_1 & \epsilon_1 \gamma_1 & \alpha_1 & \dots \\ \dots & \dots & \dots & \dots & \dots \end{vmatrix} = 0, \quad (15)$$

with the definition

$$\alpha_m(\omega, k) \equiv \epsilon_0 \gamma_m(\omega) - k^2 c^2. \quad (16)$$

This condition renders the allowed propagation wave vectors  $k$  for a given  $\omega$ , that is, the dispersion relation. A word of caution:  $\epsilon_0$  in Eq. (16) is the Fourier coefficient  $n=0$  of the dielectric constant  $\epsilon(t)$  [Eq. (11)] and should not be confused with the vacuum permittivity  $\epsilon_o$  in Eq. (4). From the fact that  $\gamma_m(\omega + \Omega) = \gamma_{m-1}(\omega)$  and  $\alpha_m(\omega + \Omega) = \alpha_{m-1}(\omega)$ , and the inspection of Eq. (15), we reach the conclusion that

$$k(\omega + \Omega) = k(\omega). \quad (17)$$

This has an important implication, namely, that *the photonic band structure is periodic in  $\omega$* , the period being the modulation frequency  $\Omega$ . The corresponding generic band structure is displayed in Fig. 1. It is significant that, for a given  $\omega$ , Eq. (15) has solutions for an infinite number of  $k$ 's (as is also apparent from Fig. 1). Denoting one of these as  $k=k_p$ , Eqs. (10) and (12) must be modified as

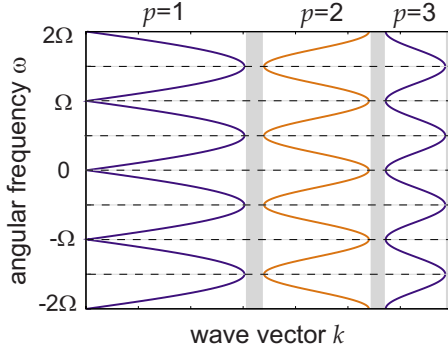


FIG. 1. (Color online) Generic dispersion curves  $\omega(k)$  for a time-periodic dielectric constant  $\epsilon(t)$ . The dispersion curves are periodic along the frequency axis with period  $\Omega$ . There are allowed ( $p=1,2,3,\dots$ ) and forbidden (gray regions) bands. The dashed lines are the “mirror planes.”

$$E_p(\omega, t) = \bar{E}_p(\omega, t) e^{-i\omega t} \quad (18)$$

and

$$\bar{E}_p(\omega, t) = \sum_n e_{pn}(\omega) e^{in\Omega t}. \quad (19)$$

Here, the coefficients  $e_{pn}(\omega)$  are the amplitudes of the harmonics  $\omega - n\Omega$  ( $n=0, \pm 1, \pm 2, \dots$ ) which are determined from the set (13), but now they are normalized in some convenient manner (for example, for a chosen integer  $n=n_o$ ,  $e_{pn_o}=1$ ). Since the dispersion relation [Eq. (15)] gives rise to a band structure [see Fig. 1], the  $p$  index can also define the serial band number ( $p=1, 2, \dots$ ). In this modified representation, we rewrite Eq. (13) as

$$\sum_n [\gamma_m(\omega) \epsilon_{m-n} - k_p^2(\omega) c^2 \delta_{mn}] e_{pn}(\omega) = 0, \quad (20)$$

$$m, n = 0, \pm 1, \pm 2, \dots, \quad p = 1, 2, \dots$$

The orthogonality and closure relation of the modes  $E_p(\omega, t)$  ( $p=1, 2, \dots$ ) are presented in Appendix B. The single plane wave [Eq. (8)] must then be replaced by a superposition of plane waves for all the possible wave vectors  $k_p(\omega)$ , namely, using Eqs. (18) and (19),

$$E(y, t) = \sum_{p=1}^{\infty} A_p E_p(\omega, t) e^{ik_p(\omega)y} = \sum_{p=1}^{\infty} \sum_{n=-\infty}^{\infty} A_p e_{pn}(\omega) e^{i[k_p(\omega)y - (\omega - n\Omega)t]}. \quad (21)$$

We note that Eq. (21) is a superposition of the normalized electric field eigenfunctions; while the  $e_{pn}(\omega)$  are the solutions of the eigenvalue problem defined by Eq. (20), the  $A_p$  are arbitrary constants for the bulk. If, on the other hand, the excitation mechanism—such as an incident plane wave [see Sec. III]—is specified, then the amplitudes  $A_p$  will, necessarily, be uniquely determined. We also mention that negative frequencies [ $\omega - n\Omega = -|\omega - n\Omega|$ ] in the phase of a partial wave in Eq. (21) can occur. In this case, this partial wave propagates in the negative  $y$  direction, for

$$e^{i[ky - (\omega - n\Omega)t]} = e^{i[ky + |\omega - n\Omega|t]}.$$

Therefore, in general, wave harmonics propagating in both the positive and negative  $y$  directions can be excited when the dielectric constant is a function of the time.

### C. Band structure

Next, we analyze the behavior of  $k_p(\omega)$  and  $e_{pn}(\omega)$  upon the increment of  $\omega$  by  $r\Omega$  where  $r$  is an integer. For  $\omega \rightarrow \omega + r\Omega$ , the eigenvalue equation [Eq. (20)] becomes

$$\sum_n [\gamma_m(\omega + r\Omega) \epsilon_{m-n} - k_p^2(\omega + r\Omega) c^2 \delta_{mn}] e_{pn}(\omega + r\Omega) = 0. \quad (22)$$

As stated before,  $\gamma_m(\omega + r\Omega) = \gamma_{m-r}(\omega)$  and  $k_p(\omega + r\Omega) = k_p(\omega)$  [see Eq. (17)]. First, we substitute this into Eq. (22) and second, we transform the indices  $m, n$  of this equation as  $m \rightarrow m+r$  and  $n \rightarrow n+r$ , respectively. Thus, we obtain

$$\sum_n [\gamma_m(\omega) \epsilon_{m-n} - k_p^2(\omega) c^2 \delta_{mn}] e_{p, n+r}(\omega + r\Omega) = 0. \quad (23)$$

By comparing Eqs. (20) and (23), we can realize that

$$e_{pn}(\omega + r\Omega) = e_{p, n-r}(\omega). \quad (24)$$

Also, it is concluded from Eqs. (17) and (24) that only the solution for a selected  $\omega$  is needed to obtain the solution for any harmonic  $\omega + r\Omega$  ( $r$  being an integer). In particular, without loss of information, the frequency can be restricted to the interval  $0 < \omega \leq \Omega$ .

Further, substitution of Eq. (24) into Eqs. (19) and (18) gives that

$$\bar{E}_p(\omega + r\Omega, t) = \bar{E}_p(\omega, t) e^{ir\Omega t}, \quad E_p(\omega + r\Omega, t) = E_p(\omega, t). \quad (25)$$

This proves that the bulk electric field  $E_p$  is periodic in  $\omega$ , with period  $\Omega$ .

The band structure is symmetric about any integer multiple of  $\Omega/2$ . That is,

$$k(r\Omega/2 + \omega) = k(r\Omega/2 - \omega), \quad (26)$$

where  $r$  is an integer. We prove this in Appendix C. From this property of symmetry, it immediately follows that  $k$  must have a maximum or a minimum at  $r\Omega/2$  for all the  $k$  bands. Therefore the slope  $d\omega/dk$  must be infinite, that is,

$$\left. \frac{d\omega}{dk_p} \right|_{\omega=r\Omega/2} = \pm \infty, \quad p = 1, 2, 3, \dots \quad (27)$$

Then Eqs. (17) and (27) imply that intervals are formed between maximum and minimum values of  $k$  that are forbidden for propagation, namely, the band gaps ( $k$  gaps) in the band structure or dispersion relation. According to these general characteristics, in Fig. 1 we illustrate qualitatively the band structure  $\omega(k)$  for a periodic dielectric constant  $\epsilon(t)$ .

Finally, we consider the case  $\omega \ll \Omega$  and  $k \ll \Omega/c$  (long-wavelength limit). In this limit, the wave vector  $k$  lies in the first branch  $p=1$  and the dispersion relation becomes linear, that is, of the form

$$k_1(\omega) = \frac{\omega}{c} \sqrt{\tilde{\epsilon}}. \quad (28)$$

It turns out that  $\tilde{\epsilon}$  is given by

$$\frac{1}{\tilde{\epsilon}} = \frac{1}{T} \int_0^T \frac{dt}{\epsilon(t)}, \quad (29)$$

as is proved in Appendix D. Of course, because of the periodicity of  $k_1(\omega)$ , the slope  $d\omega/dk_1$  is still given by  $c/\sqrt{\tilde{\epsilon}}$  also for the frequencies  $\omega + r\Omega$  ( $r=1, 2, \dots$ ) as long as  $\omega \ll \Omega$ .

#### D. Density of states

If we take into account the finite volume  $V$  occupied by the dielectric, then application of the periodic boundary conditions leads to  $V/(8\pi^3)$  modes per unit volume in the  $k$  space. Then, in a spherical shell of radius  $k$  and width  $dk$ , there are  $[V/(8\pi^3)][4\pi k^2|dk|]$  modes of oscillation of the field. Replacing  $|dk|$  by  $d\omega/|v(\omega)|$ , where  $v(\omega) \equiv d\omega/dk$  is the group velocity, we obtain the mode density for the  $p$ th band,

$$\mathcal{D}_p(\omega) = \frac{V}{2\pi^2} \frac{k_p^2(\omega)}{|v_p(\omega)|}, \quad p = 1, 2, 3, \dots \quad (30)$$

It is important to note, as follows from Eqs. (30) and (27), that

$$\mathcal{D}_p(\Omega r/2) = 0, \quad r = 0, \pm 1, \pm 2, \dots \quad (31)$$

That is, the density of modes vanishes at all the frequencies  $\omega=0, \pm\Omega/2, \pm\Omega, \pm 3\Omega/2$ , etc. Note that for  $\omega = 0, \pm\Omega, \pm 2\Omega, \dots$ , the band  $p=1$  does not contribute to the mode density because  $k_1(\Omega r) = 0$  ( $r$  being an integer)—despite the fact that the group velocity there is finite [see Fig. 1].

### III. SLAB

#### A. General theory

We consider a slab that occupies the region  $0 < y < L$  and that has a time-periodic dielectric function  $[\epsilon(t) = \epsilon(t+T)]$ . The dielectric constant of the medium for  $y < 0$  [ $y > L$ ] is  $\epsilon_1$  [ $\epsilon_2$ ]. We assume that a plane wave coming from  $y < -\infty$  with angular frequency  $\omega_o$  strikes the interface at normal incidence (see Fig. 2). Hereafter, without loss of generality, the electric (magnetic) field has only a  $z(x)$  component.

The electromagnetic fields for the incident wave are

$$E_{\text{inc}}(y, t) = E_o e^{i[k_o(\omega_o)y - \omega_o t]}, \quad (32)$$

$$H_{\text{inc}}(y, t) = H_o e^{i[k_o(\omega_o)y - \omega_o t]}. \quad (33)$$

Here,  $k_o(\omega_o) \equiv \sqrt{\epsilon_1} \omega_o / c$  and  $E_{\text{inc}}(y, t)$  and  $H_{\text{inc}}(y, t)$  are the electric and magnetic fields with their corresponding amplitudes  $E_o$  and  $H_o$ , respectively. We consider that the electric and magnetic fields inside the slab are superpositions of the normal modes as

$$E_{\text{sl}}(y, t) = \sum_{p=1}^{\infty} \sum_{n=-\infty}^{\infty} [A_p e^{ik_p(\omega_o)y} + B_p e^{-ik_p(\omega_o)y}] e_{pn}(\omega_o) e^{-i(\omega_o - n\Omega)t}, \quad (34)$$

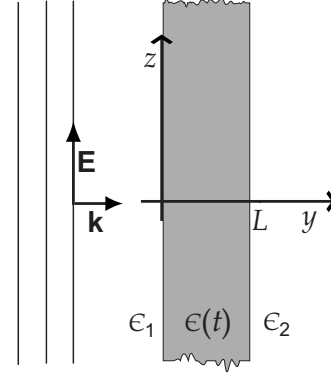


FIG. 2. Reflection and transmission of a plane wave incident on a slab with time-periodic dielectric constant  $\epsilon(t)$ .

$$H_{\text{sl}}(y, t) = \sum_{p=1}^{\infty} \sum_{n=-\infty}^{\infty} [C_{pn} e^{ik_p(\omega_o)y} + D_{pn} e^{-ik_p(\omega_o)y}] e_{pn}(\omega_o) e^{-i(\omega_o - n\Omega)t}. \quad (35)$$

We recall that  $\Omega \equiv 2\pi/T$  and  $e_{pn}$  are the eigenfunctions. The incident field excites waves with wave vectors  $k_p(\omega_o)$  that correspond to all the  $k$  bands ( $p=1, 2, 3, \dots$ ) and all harmonics  $\omega_o - n\Omega$  ( $n=0, \pm 1, \pm 2, \dots$ ). The reflected and transmitted fields are superpositions of waves with the frequency harmonics  $\omega_o - n\Omega$  generated in the dynamic slab. The reflected field is

$$E_r(y, t) = \sum_n E_n^r e^{-i[k_n^r(\omega_o)y + (\omega_o - \Omega n)t]}, \quad (36)$$

$$H_r(y, t) = - \sum_n H_n^r e^{-i[k_n^r(\omega_o)y + (\omega_o - \Omega n)t]}, \quad (37)$$

whereas the transmitted field is

$$E_t(y, t) = \sum_n E_n^t e^{i[k_n^t(\omega_o)(y-L) - (\omega_o - \Omega n)t]}, \quad (38)$$

$$H_t(y, t) = \sum_n H_n^t e^{i[k_n^t(\omega_o)(y-L) - (\omega_o - \Omega n)t]}. \quad (39)$$

Here  $k_n^{r,t}(\omega_o) = \sqrt{\epsilon_{1,2}}(\omega_o - \Omega n)/c$  is the wave vector for each of the reflected (transmitted) harmonics. From the Maxwell equations, we obtain that

$$H_o = \sqrt{\frac{\epsilon_o \epsilon_1}{\mu_o}} E_o, \quad H_n^{r,t} = \sqrt{\frac{\epsilon_o \epsilon_{1,2}}{\mu_o}} E_n^{r,t},$$

$$\begin{bmatrix} C_{pn} \\ D_{pn} \end{bmatrix} = \sqrt{\frac{\epsilon_o}{\mu_o} \frac{k_p(\omega_o)c}{\omega_o - \Omega n}} \begin{bmatrix} A_p \\ -B_p \end{bmatrix}. \quad (40)$$

The boundary conditions at the interfaces ( $y=0$  and  $y=L$ ) should determine the amplitudes  $E_n^t$ ,  $E_n^r$ ,  $A_p$ , and  $B_p$ . These conditions are

$$E_{\text{inc}}(0, t) + E_r(0, t) = E_{\text{sl}}(0, t), \quad (41)$$

$$H_{\text{inc}}(0, t) + H_r(0, t) = H_{\text{sl}}(0, t), \quad (42)$$

$$E_{\text{sl}}(L, t) = E_t(L, t), \quad (43)$$

$$H_{\text{sl}}(L, t) = H_t(L, t). \quad (44)$$

These boundary conditions and the coefficient relationships [Eq. (40)] render four sets of linear equations with the free index  $n$  taking all integer values, namely,

$$E_o \delta_{n0} + E_n^r = \sum_p e_{pn}(\omega_o)[A_p + B_p], \quad (45)$$

$$E_o \sqrt{\epsilon_1} \delta_{n0} - E_n^r \sqrt{\epsilon_1} = \sum_p \frac{e_{pn}(\omega_o) k_p(\omega_o) c}{\omega_o - n\Omega} [A_p - B_p], \quad (46)$$

$$E_n^t = \sum_p e_{pn}(\omega_o)[A_p e^{ik_p(\omega_o)L} + B_p e^{-ik_p(\omega_o)L}], \quad (47)$$

$$E_n^t \sqrt{\epsilon_2} = \sum_p \frac{e_{pn}(\omega_o) k_p(\omega_o) c}{\omega_o - n\Omega} [A_p e^{ik_p(\omega_o)L} - B_p e^{-ik_p(\omega_o)L}]. \quad (48)$$

Clearly, Eqs. (46) and (48) fail if  $\omega_o$  happens to be an integer multiple of  $\Omega$ . For this case  $\omega_o = N\Omega$  [ $N=1, 2, 3, \dots$ ], while sets (46) and (48) are still valid for  $n \neq N$ , they must be modified as follows for  $n=N$ :

$$\sum_p e_{pN}(\omega_o) k_p(\omega_o) c [A_p - B_p] = 0, \quad (49)$$

$$\sum_p e_{pN}(\omega_o) k_p(\omega_o) c [A_p e^{ik_p(\omega_o)L} - B_p e^{-ik_p(\omega_o)L}] = 0. \quad (50)$$

It is evident that this slab, when illuminated by a plane harmonic wave, essentially becomes a *polychromatic* source of light, radiating at all the harmonics  $|\omega_o - \Omega n|$ . We thus established the general equations needed to determine the electric field reflection and transmission coefficients of the generated harmonics  $\omega - n\Omega$  [ $n=0, \pm 1, \pm 2, \dots$ ].

### B. Poynting vector

As a direct consequence of the Maxwell equations [Eq. (4)], the Poynting theorem in its usual form is still valid for the case in which the dielectric constant depends on time. Because the responses  $\mathbf{D}(\mathbf{E})$  and  $\mathbf{B}(\mathbf{H})$  are linear, the temporal rate of change in the electromagnetic energy density is

$$\frac{\partial u}{\partial t} = \text{Re}[\mathbf{E}] \cdot \frac{\partial}{\partial t} \text{Re}[\mathbf{D}] + \text{Re}[\mathbf{H}] \cdot \frac{\partial}{\partial t} \text{Re}[\mathbf{B}] \quad (51)$$

and the Poynting vector is

$$\mathbf{S} = \text{Re}[\mathbf{E}] \times \text{Re}[\mathbf{H}], \quad (52)$$

where  $\text{Re}[\dots]$  denotes the real part. Since the electric (magnetic) field has only a  $z(x)$  component, the Poynting vector is directed in the  $y$  direction. By using  $\text{Re}[E] = (E + E^*)/2$  and  $\text{Re}[H] = (H + H^*)/2$  in Eq. (52), we obtain that the instantaneous Poynting vector is

$$S(y, t) = S_1(y, t) + S_2(y, t), \quad (53)$$

with the definitions

$$S_1(y, t) \equiv \frac{1}{2} \text{Re}[E(y, t) H^*(y, t)], \quad (54a)$$

$$S_2(y, t) \equiv \frac{1}{2} \text{Re}[E(y, t) H(y, t)]. \quad (54b)$$

The energy flux of the transmitted wave  $S^t(y, t)$  is obtained from Eqs. (38) and (39) and the relationships [Eq. (40)]. This renders the energy flux partial contributions,

$$S_1^t(y, t) = \frac{1}{2} \sqrt{\frac{\epsilon_o \epsilon_2}{\mu_o}} \sum_{m, n=-\infty}^{\infty} \text{Re}[E_m^t E_n^{t*} e^{i\Omega(m-n)[-\sqrt{\epsilon_2}(y-L)/c+t]}], \quad (55)$$

$$S_2^t(y, t) = \frac{1}{2} \sqrt{\frac{\epsilon_o \epsilon_2}{\mu_o}} \sum_{m, n=-\infty}^{\infty} \text{Re}[E_m^t E_n^t e^{i[2\omega_o - \Omega(m+n)][\sqrt{\epsilon_2}(y-L)/c-t]}]. \quad (56)$$

A detector has a characteristic *temporal* resolution  $2\pi/\omega_{\text{cut}}$ . This means that the detector cannot respond to oscillatory components of  $S^t(y, t) = S_1^t(y, t) + S_2^t(y, t)$  whose frequencies exceed  $\omega_{\text{cut}}/(2\pi)$ . The outcome of this filtering process is the time average  $\langle S^t(y, t) \rangle$ .  $S^t(t)$  has a nonoscillatory contribution that comes from  $S_1(t)$  and may also have a nonoscillatory contribution arising from  $S_2(y, t)$  (see below). In principle, these can be detected regardless of the cutoff frequency  $\omega_{\text{cut}}$ . The nonoscillatory terms of  $S_1^t(y, t)$  [Eq. (55)] arise when  $m=n$ . Explicitly, the nonoscillatory contribution of  $S_1^t(t)$  is

$$\langle S_1^t(y, t) \rangle_{\text{nosc}} = \frac{1}{2} \sqrt{\frac{\epsilon_o \epsilon_2}{\mu_o}} \sum_{m=-\infty}^{\infty} |E_m^t|^2. \quad (57)$$

This is the sum of the individual fluxes for each of the harmonics. On the other hand, the nonoscillatory terms of  $S_2^t(y, t)$  can occur *only* in the case that  $\omega_o = \Omega N/2$  ( $N$  being an integer). If this condition is fulfilled, then the nonoscillatory terms of  $S_2(t)$  [see Eq. (56)] come from the wave mixing of harmonics satisfying  $m+n=N$ . In this case then, the nonoscillatory contribution of  $S_2^t(t)$  is

$$\langle S_2^t(y, t) \rangle_{\text{nosc}} = \frac{1}{2} \sqrt{\frac{\epsilon_o \epsilon_2}{\mu_o}} \sum_{m=-\infty}^{\infty} \text{Re}[E_m^t E_{N-m}^t], \quad \omega_o = \Omega N/2. \quad (58)$$

In addition to the aforementioned nonoscillatory contributions [Eqs. (57) and (58)], the signal measured by the detector contains terms describing beats as a consequence of the wave mixing of different frequencies. The wave mixing creates two types of beats in  $S^t(y, t)$ : (i) with frequencies  $\Omega, 2\Omega, 3\Omega, \dots$  stemming from Eq. (55) and (ii) with frequencies  $|2\omega_o|, |2\omega_o \pm \Omega|, |2\omega_o \pm 2\Omega|, \dots$ , originating from Eq. (56). No need to say, in addition to the detector's temporal resolution range, the observation of these beats would be also limited by the spectral range of the detector that is employed.

The energy flux of the reflected wave follows the same analysis as that for the transmitted wave. The energy flux expressions of the reflected wave  $S^r(y, t)$  are obtained by making the replacements  $\sqrt{\epsilon_2} \rightarrow -\sqrt{\epsilon_1}$  and  $E_m^t \rightarrow E_m^r$  and by eliminating  $L$  in Eqs. (55)–(58).

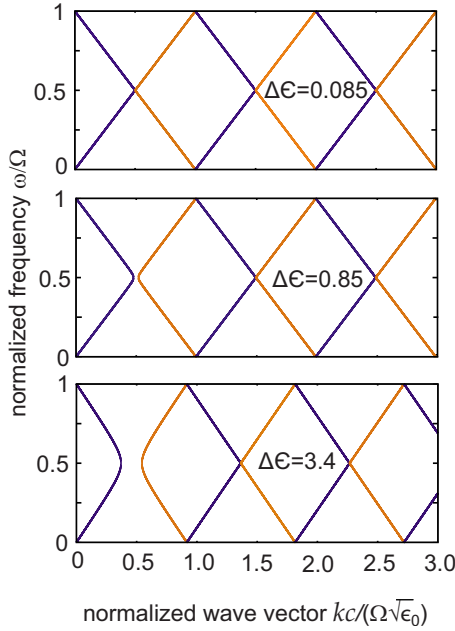


FIG. 3. (Color online) Band structures for the sinusoidal modulation of the dielectric function which correspond to weak ( $\Delta\epsilon=0.085$ ), moderate ( $\Delta\epsilon=0.85$ ), and strong ( $\Delta\epsilon=3.4$ ) modulations in Eq. (59).

#### IV. NUMERICAL SIMULATIONS

In this section we apply our theory to obtain the reflected and transmitted fields for particular cases. We assume that the medium surrounding the slab is vacuum, that is,  $\epsilon_1=\epsilon_2=1$ , and that the dielectric function of the slab is modulated sinusoidally as

$$\epsilon(t) = \epsilon_0 + \Delta\epsilon \sin(\Omega t). \quad (59)$$

We consider that  $\epsilon_0=5.25$ . This value corresponds to the dielectric constant of lithium niobate which is a material with a large electro-optical coefficient ( $r \approx 31$  pm/V). When this material is placed within two biased electrode plates (voltage  $V$  and separation  $d$ ), the change in the dielectric constant is approximately  $\Delta\epsilon \approx \epsilon_0^2 r V/d$ . For an estimate in this material, this change is on the order of  $\Delta\epsilon = 8.5 \times 10^{-4} V(\text{kV})/d(\text{mm})$ . Thus, even with large voltages and small interplate separations, it is difficult to attain large changes in the dielectric constant. Also, any material has a finite response time to an external agent. Consequently, the frequency at which the medium can be modulated is limited. For lithium niobate, the upper frequency limit is of the order of 1 GHz. Aware of these considerations, we proceed to analyze the regimes: (1) weak modulation ( $\Delta\epsilon=0.085$ ), (2) moderate modulation ( $\Delta\epsilon=0.85$ ), and (3) strong modulation ( $\Delta\epsilon=3.4$ ).

For completeness, the band structures for these cases are shown in Fig. 3. For the weak-modulation case, the widths of the forbidden  $k$  band gaps of the band structure are very small, so this band structure resembles the “empty-lattice” limit. Referring to the moderate-modulation case, the only visible difference in comparison with the previous case is that the first forbidden  $k$  band gap becomes appreciable. For the strong-modulation case, it can be seen that the width of

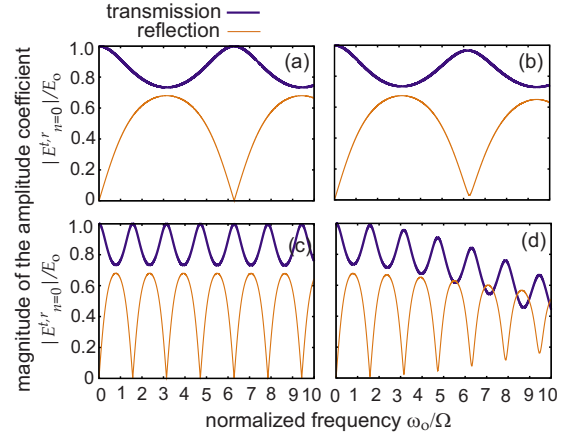


FIG. 4. (Color online) The magnitude of reflection and transmission coefficients as a function of frequency for the fundamental response ( $n=0$ ). (a) Weak modulation ( $\Delta\epsilon=0.085$ ) and  $L_N=0.5$ . (b) Moderate modulation ( $\Delta\epsilon=0.85$ ) and  $L_N=0.5$ . (c) Weak modulation ( $\Delta\epsilon=0.085$ ) and  $L_N=2$ . (d) Moderate modulation ( $\Delta\epsilon=0.85$ ) and  $L_N=2$ .

the first forbidden  $k$  band gap is remarkably increased, whereas the widths of the allowed  $k$  bands become reduced in comparison with the other cases.

Hereafter, we consider three values of the thickness of the slab. The corresponding normalized thicknesses,

$$L_N \equiv L\Omega\sqrt{\epsilon_0}/c,$$

are  $L_N=0.5, 2$ , and  $8$ . First we focus on the weak-modulation case ( $\Delta\epsilon=0.085$ ). In Figs. 4(a) and 4(c), the magnitudes of the reflection and transmission amplitude coefficients are plotted as a function of the frequency of the incident wave for the fundamental response ( $n=0$ ) with  $L_N=0.5$  and  $2$ , respectively, whereas their corresponding phases are plotted in Figs. 5(a) and 5(c). Since the modulation is weak, we expect the optical response for the fundamental to be the same as

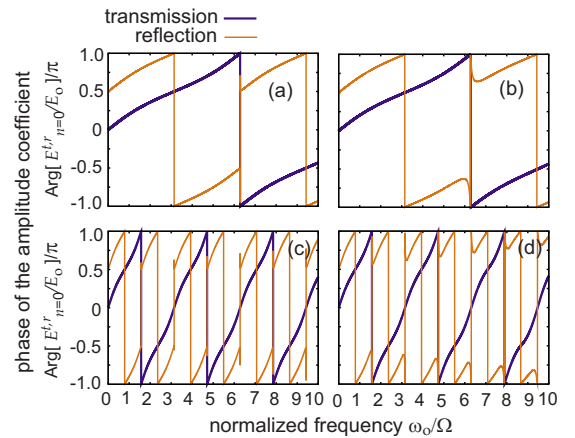


FIG. 5. (Color online) The phase of the reflection and transmission coefficients as a function of frequency for the fundamental response ( $n=0$ ). (a) Weak modulation ( $\Delta\epsilon=0.085$ ) and  $L_N=0.5$ . (b) Moderate modulation ( $\Delta\epsilon=0.85$ ) and  $L_N=0.5$ . (c) Weak modulation ( $\Delta\epsilon=0.085$ ) and  $L_N=2$ . (d) Moderate modulation ( $\Delta\epsilon=0.85$ ) and  $L_N=2$ .

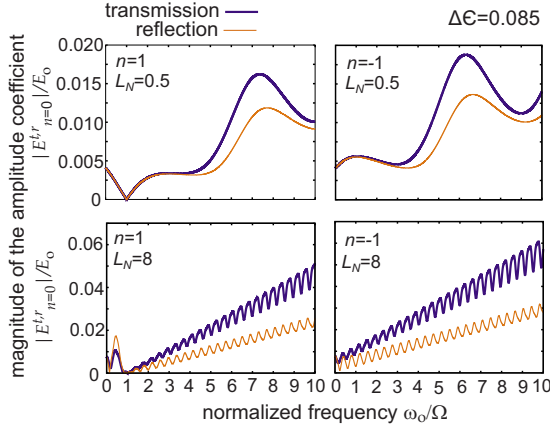


FIG. 6. (Color online) The magnitude of the reflection and transmission coefficients as a function of frequency for the weak-modulation case  $\Delta\epsilon=0.085$ , the harmonics  $n = \pm 1$ , and  $L_N=0.5, 8$ .

that for a Fabry-Perot etalon with dielectric constant  $\epsilon_0$ . Thus, in this limit

$$E_0^r/E_0 = \frac{(r_{13} + r_{32} \exp[i2\omega_o L_N/\Omega])}{(1 + r_{13}r_{32} \exp[i2\omega_o L_N/\Omega])}, \quad (60)$$

$$E_0^t/E_0 = \frac{t_{13}t_{32} \exp[i\omega_o L_N/\Omega]}{(1 + r_{13}r_{32} \exp[i2\omega_o L_N/\Omega])}, \quad (61)$$

where  $r_{ij} = (\sqrt{\epsilon_i} - \sqrt{\epsilon_j})/(\sqrt{\epsilon_i} + \sqrt{\epsilon_j})$  and  $t_{ij} = 2\sqrt{\epsilon_i}/(\sqrt{\epsilon_i} + \sqrt{\epsilon_j})$  are the Fresnel coefficients for reflection and transmission, respectively. The subscript 3 in these coefficients corresponds to the dielectric constant of the slab ( $\epsilon_0$ ). We mention that  $\omega_o L_N/\Omega$  is simply  $2\pi L/\lambda$ , where  $\lambda \equiv 2\pi c/(\sqrt{\epsilon_o}\omega_o)$ . In fact, in general the response for the fundamental  $n=0$  follows Eqs. (60) and (61). In particular, it is well known that the reflectance from a slab bounded by identical media vanishes if the slab thickness is equal to an integer multiple of one-half the wavelength in the slab. Given the fact that the near-zero reflection minima in Figs. 4(a) and 4(c) occur at frequencies  $\omega_o/\Omega = l\pi/L_N$  ( $l$  is a positive integer), it follows that these values indeed correspond to  $L = (\lambda/2)l$ . There is an exception, however, for the phase of the reflection coefficient in a very small interval around the frequencies  $\omega_o/\Omega = l\pi/L_N$  ( $l$  is a positive integer) for which Eq. (60) vanishes. While Eq. (60) predicts a phase discontinuity from  $-\pi/2$  to  $\pi/2$  at these frequencies, Figs. 5(a) and 5(c) show deviations from this phase change. Since the modulation is weak, the strengths of other harmonics ( $n \neq 0$ ) should be weak as well. This is shown in Fig. 6, where the magnitudes of the reflection and transmission amplitude coefficients are plotted as a function of the frequency for the harmonics  $n = \pm 1$ , and  $L_N=0.5$  and 8. Indeed, the strengths of these harmonics are much smaller than that of the fundamental ( $n=0$ ). We notice that the strengths of these harmonics are greater for the larger  $L_N$  shown in Fig. 6. The overall strengths of the harmonics increase as the frequency increases. Also, it happens that the reflection and transmission amplitudes for the harmonic  $n = 1$  vanish at the frequency  $\omega_o/\Omega = 1$ . On the other hand, the phases of the reflection and transmission coefficients as a

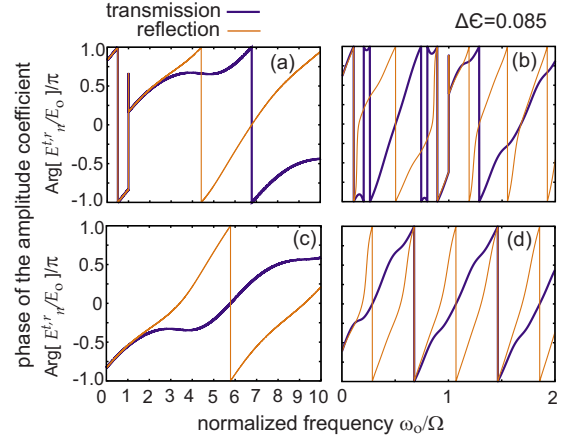


FIG. 7. (Color online) The phase of the reflection and transmission coefficients as a function of frequency for the weak-modulation ( $\Delta\epsilon=0.085$ ). (a) Harmonic  $n=1$  and  $L_N=0.5$ . (b) Harmonic  $n=1$  and  $L_N=8$ . (c) Harmonic  $n=-1$  and  $L_N=0.5$ . (d) Harmonic  $n=-1$  and  $L_N=8$ .

function of  $\omega_o/\Omega$  for the aforementioned harmonics ( $n = \pm 1$  and  $L_N=0.5$  and 8) are depicted in Fig. 7. As noticed in this figure, the phase varies faster as a function of the frequency as the thickness of the slab increases. Also, phase discontinuities in the reflection and transmission coefficients occur for the harmonic  $n=1$  at the frequency  $\omega_o/\Omega = 1$ . It is precisely at this frequency that both coefficients vanish (see Fig. 6). We encountered a similar situation at the frequencies for which the reflection coefficient for the fundamental  $n=0$  vanishes.

Next, we discuss the moderate-modulation case. As can be seen in Figs. 4(b) and 4(d), as the frequency increases, the strengths of reflection and transmission coefficients of the fundamental ( $n=0$ ) deviate from the response given by Eqs. (60) and (61). On the other hand, we can see that the phases of the transmission coefficients [Figs. 5(b) and 5(d)] are nearly equal to those for the weak modulation [Figs. 5(a) and 5(c)]. However, the phases of the reflection coefficient are different in comparison with the previous case in the intervals around the frequencies  $\omega_o/\Omega = l\pi/L_N$  ( $l$  is a positive integer). On the other hand, the strengths of the reflection and transmission coefficients for the harmonics  $n = \pm 1$ , as a function of the frequency, are qualitatively similar as those for the weak modulation (see Fig. 6), but now they are 1 order of magnitude greater (see Fig. 8). Again, the magnitudes of the reflection and transmission coefficients for the harmonic  $n=1$  vanish at the frequency  $\omega_o/\Omega = 1$ . As shown in Fig. 8, the presence of the harmonics  $n = \pm 2$  is now appreciable. As could have been expected, as the modulation amplitude  $\Delta\epsilon$  increases, the appearance of stronger harmonics occurs. The magnitudes of the reflection and transmission coefficients for  $n=2$  not only vanish at the frequency  $\omega_o/\Omega = 2$  but also at  $\omega_o/\Omega = 1$  (see Fig. 8). The corresponding phases of the reflection and transmission coefficients for the harmonics  $n = \pm 1, \pm 2$  and  $L_N=0.5$  and 8 are plotted in Fig. 9. The phases of the reflection and transmission coefficients for the harmonics  $n = \pm 1$  are almost the same as those for the weak modulation. Phase discontinuities for  $n=1$  show up at the frequency  $\omega_o/\Omega = 1$ , whereas those for  $n=2$  show up at

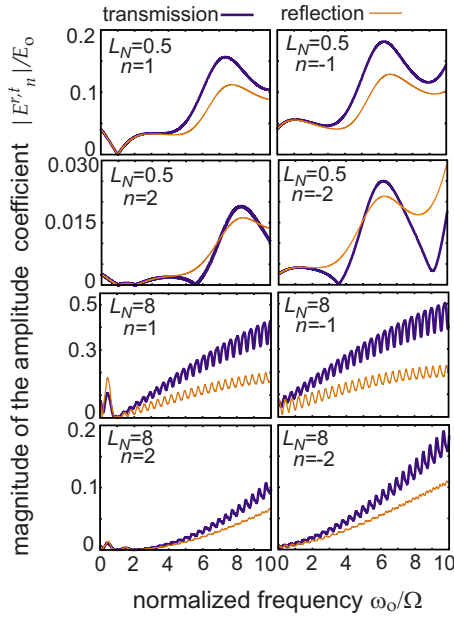


FIG. 8. (Color online) The magnitude of the reflection and transmission coefficients as a function of frequency for the moderate-modulation case  $\Delta\epsilon=0.85$ , the harmonics  $n=\pm 1, \pm 2$ , and  $L_N=0.5$  and 8.

the frequencies  $\omega_0/\Omega=1, 2$ . These discontinuities occur at the frequencies for which the magnitudes of the reflection and transmission coefficients vanish.

Finally, we deal with the strong-modulation case. In Fig. 10 (Fig. 11), the strengths (phases) of the reflection and transmission coefficients for the harmonics  $n=0, \pm 1, \pm 2, \pm 3, -4$  and  $L_N=0.5, 2$ , and 8 are shown. By comparing the plots of the magnitudes and phases for the

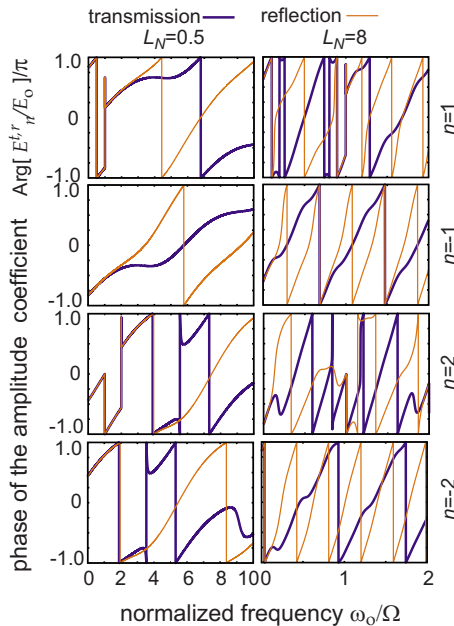


FIG. 9. (Color online) The phase of the reflection and transmission coefficients as a function of frequency for the moderate-modulation case  $\Delta\epsilon=0.85$ , the harmonics  $n=\pm 1, \pm 2$ , and  $L_N=0.5$  and 8.

three different thicknesses of the slab, we note that they are very unlike. Also, the strength of the reflected and transmitted harmonics for higher orders becomes comparable with the ones for lower orders. The smoothness of the plots decreases as  $L_N$  increases. However, for  $L_N=8$ , the fast variation in the strengths of the reflection and transmission harmonics seems to follow a smooth envelope. The strength of the reflected and transmitted harmonics is similar for  $L_N=0.5$  and 2, whereas for  $L_N=8$  the strengths of some harmonics exceed one. This happens for the transmitted fundamental  $n=0$  and for the reflected harmonics  $n=0, 1$  [see Fig. 10(c)]. This is not surprising since the dynamic slab serves as an agent to couple and to transfer energy between different harmonics. Since the system is open, the reflected and transmitted energy is provided in part by the external agent that modulates the dynamic medium. According to the plots in Figs. 6, 8, and 10, we can infer that the magnitudes of the reflection and transmission coefficients for a given positive harmonic  $n_o$  vanish at the frequencies  $\omega_0/\Omega=1, 2, \dots, n_o$ ; the phases are discontinuous at these frequencies.

## V. CONCLUSIONS

We established a general theory of propagation of electromagnetic waves in a bulk medium with a dielectric function  $\epsilon(t)$  that is periodic in time, namely, modulated at a frequency  $\Omega$ . We derived and analyzed in detail the dispersion relation  $\omega(k)$  and the propagating modes. The dispersion relation takes the form of a band structure that is periodic in the frequency and has forbidden band gaps for the wave vector. Also, we analyzed the general properties of the band structure. Further, we derived a general formalism to describe the response of a dynamic-periodic slab when illuminated by a monochromatic wave (frequency  $\omega_0$ ) at normal incidence. We found that the reflected and transmitted fields are superpositions of plane waves oscillating with the frequencies  $\omega_0, \omega_0 \pm \Omega, \omega_0 \pm 2\Omega, \dots$ ; thus the slab becomes a polychromatic source. Inside the slab the incident wave excites the modes of a dynamic bulk which contain plane waves with wave vectors  $k_1(\omega_0), k_2(\omega_0), k_3(\omega_0), \dots$ , as well as the aforementioned harmonics  $\omega_0 - n\Omega$ . The expressions for the Poynting vectors of the reflected and transmitted fields were also obtained. We discussed both the time-independent and time-dependent energy fluxes that can be measured by a detector. We applied the theory to the case in which the dynamic slab is sinusoidally modulated, considering three regimes of modulation: weak, moderate, and strong. The corresponding magnitudes and phases of the reflection and transmission coefficients were obtained numerically for several harmonics  $n$  and slab thicknesses  $L$ . We found that the response of the fundamental ( $n=0$ ) for weak modulation is similar as that of the Fabry-Perot etalon with dielectric constant  $\epsilon_0$ . In this regime, the strengths of the harmonics are weak. As the modulation becomes stronger, the strengths of the harmonics increase. For the strong modulation, we encountered that higher-order harmonics can be stronger than the lower-order ones for certain frequency intervals. Also, the magnitude of the reflection or the transmission coefficient can exceed one. This is a consequence of the

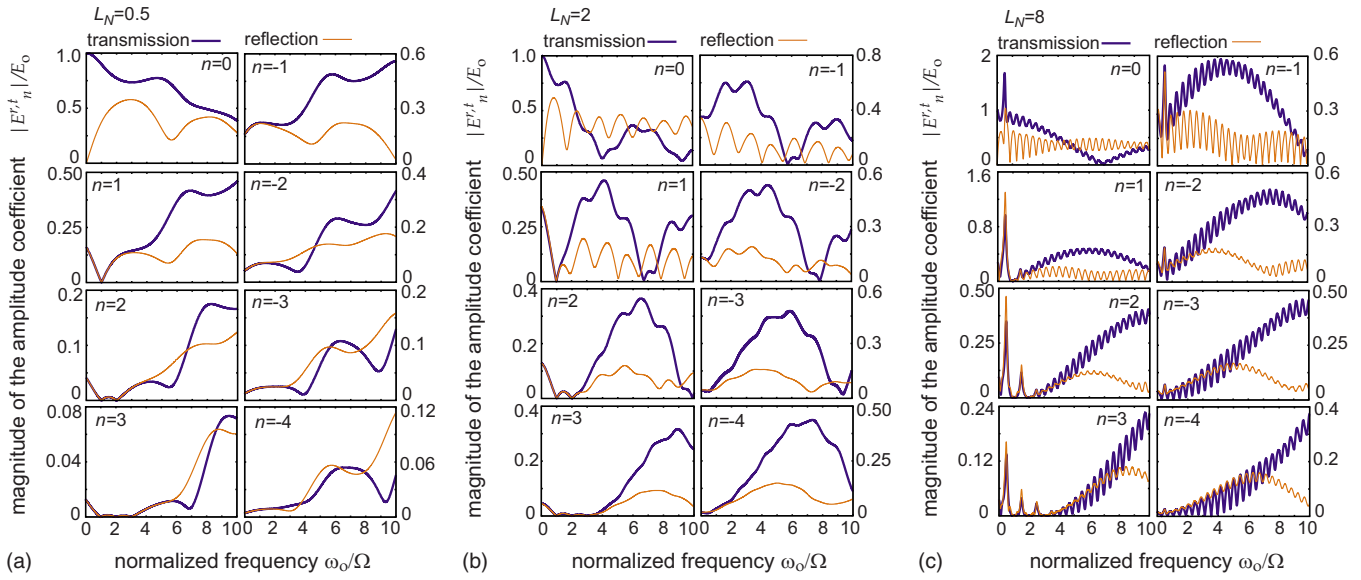


FIG. 10. (Color online) Reflection and transmission coefficients as a function of frequency for the strong-modulation case  $\Delta\epsilon=3.4$  and harmonics  $n=0, \pm 1, \pm 2, \pm 3, -4$ . (a)  $L_N=0.5$ . (b)  $L_N=2$ . (c)  $L_N=8$ .

openness of our system, namely, the external agent that modulates the slab can contribute to pumping energy into the system. Also, we found that the magnitudes of the reflection and transmission coefficients for a certain positive harmonic  $n_o$  vanish at the frequencies  $\omega_o/\Omega=1, 2, \dots, n_o$  and that their corresponding phases at these frequencies are discontinuous. Finally, since a dynamic slab generates radiation at frequencies that differ from the excitation frequency, novel devices for controlling and manipulating the propagation and radiation of electromagnetic waves, such as pulse reshaping and wavelength multiplexing in communications, could be developed. A final comment: experiments on dynamic-periodic metamaterials are now being planned at the Microwave Laboratory of our institute.

ACKNOWLEDGMENTS

P.H. is grateful to Arkady Krokhin of North Texas University for helpful discussions and wishes to acknowledge funding by the CONACyT under Project No. 79180. J.R.Z.-S. thanks the Consejo Nacional de Ciencia y Tecnología for financial support through the Repatriation Program No. 060052.

APPENDIX A: CONTINUITY CONDITIONS (ABRUPT STEP)

Herein, we derive the continuity conditions for an abrupt steplike change in  $\epsilon(t)$  at a certain time  $t_o$ . We integrate Eqs.

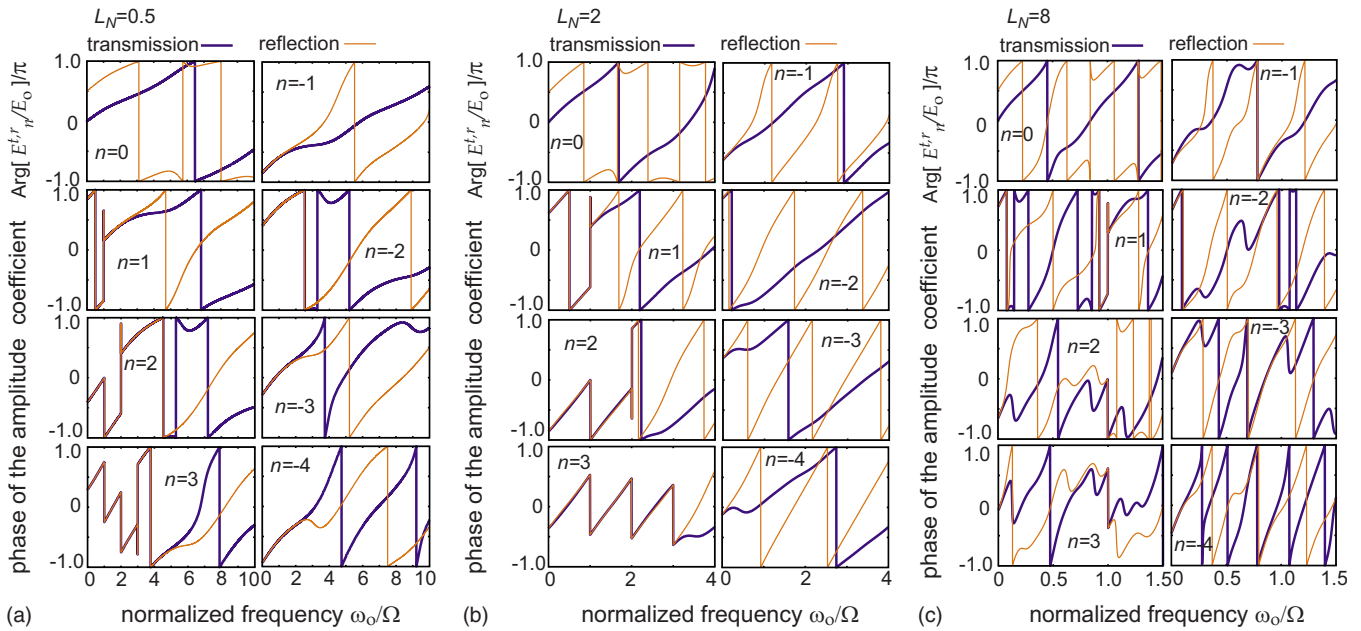


FIG. 11. (Color online) The phase of the reflection and transmission coefficients as a function of frequency for the strong-modulation case  $\Delta\epsilon=3.4$  and harmonics  $n=0, \pm 1, \pm 2, \pm 3, -4$ . (a)  $L_N=0.5$ . (b)  $L_N=2$ . (c)  $L_N=8$ .

(4c) and (4d) over the time interval  $(t_o^-, t_o^+)$  where  $t_o^\pm = t_o \pm \Delta t$  ( $\Delta t > 0$ ), thus

$$\nabla \times \left( \int_{t_o^-}^{t_o^+} \mathbf{E} dt \right) = -\mu_o \int_{t_o^-}^{t_o^+} \frac{\partial \mathbf{H}}{\partial t} dt = -\mu_o [\mathbf{H}(t_o^+) - \mathbf{H}(t_o^-)], \quad (\text{A1})$$

$$\begin{aligned} \nabla \times \left( \int_{t_o^-}^{t_o^+} \mathbf{H} dt \right) &= \int_{t_o^-}^{t_o^+} \frac{\partial}{\partial t} [\epsilon_o \epsilon(t) \mathbf{E}] dt \\ &= \epsilon_o [\epsilon(t_o^+) \mathbf{E}(t_o^+) - \epsilon(t_o^-) \mathbf{E}(t_o^-)]. \end{aligned} \quad (\text{A2})$$

In the limit  $\Delta t \rightarrow 0$ ,  $t_o^+$  and  $t_o^-$  approach  $t_o$ , and the left-hand sides of Eqs. (A1) and (A2) vanish. Consequently, the continuity conditions,

$$\mathbf{H}(t_o^+) = \mathbf{H}(t_o^-), \quad (\text{A3})$$

$$\epsilon_o \epsilon(t_o^+) \mathbf{E}(t_o^+) = \epsilon_o \epsilon(t_o^-) \mathbf{E}(t_o^-), \quad (\text{A4})$$

are established. The continuity condition for the magnetic field  $\mathbf{H}$  [Eq. (A3)] is due to the medium being nonmagnetic. From Eq. (A4) it is noticed that the displacement field  $\mathbf{D}(t) = \epsilon_o \epsilon(t) \mathbf{E}$  is continuous at the step change; thus the electric field  $\mathbf{E}$  becomes discontinuous.

## APPENDIX B: ORTHOGONALITY OF THE EIGENFUNCTIONS

To analyze the orthogonality of the eigenfunctions, we recognize that the wave equation [Eq. (9)] is a particular case of the Sturm-Liouville eigenvalue problem,

$$\mathcal{L}E(t) + \lambda w(t)E(t) = 0, \quad (\text{B1})$$

where  $\mathcal{L}$  is the self-adjoint operator defined as

$$\mathcal{L} \equiv \frac{d}{dt} \left[ q_1(t) \frac{d}{dt} \right] + q_2(t). \quad (\text{B2})$$

Here,  $q_1(t)$  and  $q_2(t)$  are arbitrary functions,  $\lambda$  are the eigenvalues, and  $w(t)$  is a weight function. Equation (9) rewritten as in Eq. (B1) becomes

$$\frac{d}{dt} \left[ \epsilon^2(t) \frac{d}{dt} E(t) \right] + \epsilon(t) \frac{d^2 \epsilon(t)}{dt^2} E(t) + (kc)^2 \epsilon(t) E(t) = 0. \quad (\text{B3})$$

Comparing with Eqs. (B1) and (B2), we can make the identifications

$$q_1(t) = \epsilon^2(t), \quad q_2(t) = \epsilon(t) \frac{d^2 \epsilon(t)}{dt^2}, \quad \lambda = (kc)^2, \quad w(t) = \epsilon(t).$$

Then, the Sturm-Liouville theory establishes that the eigenvalues  $k^2 c^2$  are real, the eigenfunctions are orthogonal with respect to the weight function  $\epsilon(t)$ , and the eigenfunctions form a complete basis. Thus, the orthogonality condition becomes

$$\int_{-\infty}^{\infty} \epsilon(t) \bar{E}_p(\omega, t) e^{-i\omega t} \bar{E}_q^*(\omega', t) e^{i\omega' t} dt = 2\pi \mathcal{N}_p^2 \delta(\omega - \omega') \delta_{pq}, \quad (\text{B4})$$

where  $\mathcal{N}_p$  is a normalizing constant. By the properties of the Bloch solution [Eq. (10)], Eq. (B4) can be simplified. First, the integral in Eq. (B4) that runs for all  $t$  can be reduced to the interval  $(0, T)$  as

$$\begin{aligned} \int_0^T \epsilon(t) \bar{E}_p(\omega, t) \bar{E}_q^*(\omega', t) e^{-i(\omega - \omega')t} dt &= \sum_{n=-\infty}^{\infty} e^{-i(\omega - \omega')nT} \\ &= 2\pi \mathcal{N}_p^2 \delta(\omega - \omega') \delta_{pq}. \end{aligned} \quad (\text{B5})$$

The sum in Eq. (B5) is equal to  $2\pi \delta(\omega - \omega')/T$ , whence

$$\frac{1}{T} \int_0^T \epsilon(t) \bar{E}_p(\omega, t) \bar{E}_q^*(\omega, t) dt = \mathcal{N}_p^2 \delta_{pq}. \quad (\text{B6})$$

This is the orthogonality condition for the periodic part of the electric field eigenfunctions. If  $\mathcal{N}_p \neq 1$  then, by dividing the eigenfunctions  $\bar{E}_p(\omega, t)$  by  $\mathcal{N}_p$ , they become normalized. Consequently, an orthonormal set of eigenfunction can be defined.

By using the Fourier expansions of  $\epsilon(t)$  and  $\bar{E}_p(\omega, t)$ , namely, Eqs. (11) and (19), respectively, Eq. (B6) reduces to

$$\frac{1}{T} \sum_{lmn} \epsilon_l e_{pm}(\omega) e_{qn}^*(\omega) \int_0^T e^{i\Omega(l+m-n)t} dt = \mathcal{N}_p^2 \delta_{pq}. \quad (\text{B7})$$

Finally,

$$\sum_{mn} \epsilon_{n-m} e_{pm}(\omega) e_{qn}^*(\omega) = \mathcal{N}_p^2 \delta_{pq}. \quad (\text{B8})$$

Equation (B8) is the condition of orthogonality in terms of the Fourier coefficients of  $\epsilon(t)$  and  $\bar{E}_p(\omega, t)$ .

The closure or completeness relation may also be derived. To do so, we express the Dirac delta function  $\delta(t - t')$  as a superposition of the eigenfunctions, that is,

$$\delta(t - t') = \int_0^\Omega \sum_p C_p(\omega, t') \bar{E}_p(\omega, t) e^{-i\omega t} d\omega. \quad (\text{B9})$$

Here,  $C_p(\omega, t')$  is the constant to be determined. First we multiply Eq. (B9) by  $\epsilon(t) \bar{E}_q^*(\omega', t) \exp(i\omega' t)$  and we integrate with respect to  $t$ . Then we apply orthogonality condition (B4), and we obtain that

$$C_p(\omega, t') = \frac{1}{2\pi \mathcal{N}_p^2} \epsilon(t') e^{i\omega t'} \bar{E}_p^*(\omega, t'). \quad (\text{B10})$$

Thus, by substituting Eq. (B10) into Eq. (B9), the closure becomes

$$\sum_p \mathcal{N}_p^{-2} \epsilon(t') \int_0^\Omega \bar{E}_p(\omega, t) \bar{E}_p^*(\omega, t') e^{-i\omega(t-t')} d\omega = 2\pi \delta(t - t'). \quad (\text{B11})$$

**APPENDIX C: SYMMETRY AROUND A MULTIPLE INTEGER OF  $\Omega/2$ : Proof of Eq. (26)**

We define  $\omega_1 \equiv (r\Omega/2 + \omega)$  and  $\omega_2 \equiv (r\Omega/2 - \omega)$ . It is straightforward to obtain from Eq. (14) that

$$\gamma_m(\omega_2) = \gamma_{r-m}(\omega_1). \quad (\text{C1})$$

Equation (20) for the frequency  $\omega_2$  becomes

$$\sum_n [\gamma_m(\omega_2)\epsilon_{m-n} - k_p^2 c^2 \delta_{mn}] e_{pn}(\omega_2) = 0. \quad (\text{C2})$$

Next, we substitute Eq. (C1) into Eq. (C2) and use the fact that  $\omega_2 = -\omega_1 + r\Omega$ . Thus Eq. (C2) becomes

$$\sum_n [\gamma_{r-m}(\omega_1)\epsilon_{m-n} - k_p^2 c^2 \delta_{mn}] e_{pn}(-\omega_1 + r\Omega) = 0. \quad (\text{C3})$$

Further, we transform the dummy indices  $m$  and  $n$  as  $m \rightarrow r-m$  and  $n \rightarrow r-n$ , respectively, in Eq. (C3). As a consequence,

$$\sum_n [\gamma_m(\omega_1)\epsilon_{-(m-n)} - k_p^2 c^2 \delta_{mn}] e_{p,r-n}(-\omega_1 + r\Omega) = 0. \quad (\text{C4})$$

By using the periodicity property given by Eq. (24) and taking the complex conjugate, we obtain that

$$\sum_n [\gamma_m(\omega_1)\epsilon_{-(m-n)}^* - k_p^2 c^2 \delta_{mn}] e_{p(-n)}^*(-\omega_1) = 0. \quad (\text{C5})$$

Now,  $\epsilon_{-(m-n)}^* = \epsilon_{m-n}$  because  $\epsilon(t)$  is a real function so Eq. (C5) becomes

$$\sum_n [\gamma_m(\omega_1)\epsilon_{m-n} - k_p^2 c^2 \delta_{mn}] e_{p,-n}^*(-\omega_1) = 0. \quad (\text{C6})$$

A comparison of Eq. (C6) with Eq. (20) for the frequency  $\omega_1$  renders  $e_{p,-n}^*(-\omega_1) = e_{pn}(\omega_1)$  (up to a multiplicative constant). Therefore, comparing Eqs. (C2) and (C6), the frequencies  $\omega_1 = r\Omega/2 + \omega$  and  $\omega_2 = r\Omega/2 - \omega$  yield the same eigenvalues  $k_p$ , which proves the symmetry property Eq. (26).

**APPENDIX D: LINEAR DISPERSION SLOPE (LONG-WAVE LIMIT): PROOF OF EQ. (29)**

Herein, we show that the slope of the dispersion relation  $\omega(k)$  of the first band ( $p=1$ ) in the long-wavelength limit [Eq. (28)] is given by Eq. (29). We use the displacement field  $\mathbf{D}$  instead of the electric field  $\mathbf{E}$ . Also,  $\mathbf{D}$  is a transverse vector and has a plane wave solution as Eq. (8) where we need only to replace  $E$  by  $D$ . From Maxwell's equations [Eq. (4)], the wave equation for the displacement field is

$$\frac{d^2 D(t)}{dt^2} + k^2 c^2 \eta(t) D(t) = 0, \quad (\text{D1})$$

where  $\eta(t) \equiv 1/\epsilon(t)$ . We represent  $D(t)$  and  $\eta(t)$  by their Fourier series representation

$$D(t) = \sum_n D_n \exp[-i(\omega - n\Omega)t], \quad (\text{D2})$$

$$\eta(t) = \sum_n \eta_n \exp[in\Omega t]. \quad (\text{D3})$$

Substituting into Eq. (D1), we obtain the linear equation set,

$$(\omega - m\Omega)^2 D_m = k^2 c^2 \sum_n \eta_{m-n} D_n, \quad m, n = 0, \pm 1, \pm 2 \dots \quad (\text{D4})$$

We consider the limits  $\omega, k \rightarrow 0$ . The first step is to express the Fourier coefficient  $D_0$  in terms of the other coefficients  $D_m$ ,  $m \neq 0$ ,

$$D_0 = \frac{1}{\eta_{ef} - \eta_{0n \neq 0}} \sum \eta_{-n} D_n. \quad (\text{D5})$$

In the last equation, we use the fact that

$$\lim_{\omega, k \rightarrow 0} \omega^2 / (k^2 c^2) = \tilde{\eta} \equiv 1/\tilde{\epsilon}, \quad (\text{D6})$$

since, for very low frequencies,  $k$  is a linear function of  $\omega$  [see Eq. (28)]. On the other hand, in the limit  $\omega, k \rightarrow 0$  for  $m \neq 0$ , Eq. (D4) becomes

$$\lim_{k \rightarrow 0} \frac{(m\Omega)^2}{(kc)^2} D_m = \eta_m D_0 + \sum_{n \neq 0} \eta_{m-n} D_n. \quad (\text{D7})$$

Substituting Eq. (D5) into Eq. (D7), we get

$$\lim_{k \rightarrow 0} \frac{(m\Omega)^2}{(kc)^2} D_m = \sum_{n \neq 0} \left[ \frac{\eta_m \eta_{-n}}{\tilde{\eta} - \eta_0} + \eta_{m-n} \right] D_n. \quad (\text{D8})$$

Notice that the left-hand side of Eq. (D8) diverges. We discard the possibility that  $D_m \rightarrow 0$  for all  $m \neq 0$  because, according to Eq. (D2), the solution would correspond to a harmonic wave, that is, to a static medium. Then, it is the right-hand side of Eq. (D8) that must diverge, implying that

$$\tilde{\eta} = \eta_0. \quad (\text{D9})$$

As is well known, the Fourier coefficient  $\eta_0$  is equal to the average, over a period, of the function that is expanded, hence

$$\tilde{\eta} = \frac{1}{T} \int_0^T \eta(t) dt. \quad (\text{D10})$$

This is the result that we set out to demonstrate [Eq. (29)].

- [1] F. R. Morgenthaler, IRE Trans. Microwave Theory Tech. **6**, 167 (1958).
- [2] D. E. Holberg and K. S. Kunz, IEEE Trans. Antennas Propag. **14**, 183 (1966).
- [3] F. A. Harfoush and A. Taflove, IEEE Trans. Antennas Propag. **39**, 898 (1991).
- [4] E. Yablonovitch, Phys. Rev. Lett. **32**, 1101 (1974).
- [5] E. Yablonovitch, Phys. Rev. Lett. **62**, 1742 (1989).
- [6] S. Juršenas, S. Miasojedovas, G. Kurilčik, A. Zukauskas, and P. R. Hageman, Appl. Phys. Lett. **83**, 66 (2003).
- [7] E. J. Reed, M. Soljacic, and J. D. Joannopoulos, Phys. Rev. Lett. **90**, 203904 (2003).
- [8] E. J. Reed, M. Soljacic, and J. D. Joannopoulos, Phys. Rev. Lett. **91**, 133901 (2003).
- [9] F. Biancalana, A. Amann, A. V. Uskov, and E. P. O'Reilly, Phys. Rev. E **75**, 046607 (2007).
- [10] W. Park and C. J. Summers, Opt. Lett. **27**, 1397 (2002).
- [11] D. Scrymgeour, N. Malkova, S. Kim, and V. Gopalan, Appl. Phys. Lett. **82**, 3176 (2003).
- [12] M. F. Yanik and S. Fan, Phys. Rev. Lett. **92**, 083901 (2004).
- [13] M. F. Yanik and S. Fan, Phys. Rev. Lett. **93**, 173903 (2004).
- [14] M. F. Yanik, W. Suh, Z. Wang, and S. Fan, Phys. Rev. Lett. **93**, 233903 (2004).
- [15] Y. A. Vlasov, M. O'Boyle, H. F. Hamann, and S. J. McNab, Nature (London) **438**, 65 (2005).
- [16] M. Notomi and S. Mitsugi, Phys. Rev. A **73**, 051803(R) (2006).
- [17] R. Soref and B. Bennett, IEEE J. Quantum Electron. **23**, 123 (1987).
- [18] C. Z. Zhao, E. K. Liu, G. Z. Li, Y. Gao, and C. S. Guo, Opt. Lett. **21**, 1664 (1996).
- [19] P. Halevi and F. Ramos-Mendieta, Phys. Rev. Lett. **85**, 1875 (2000).
- [20] S. W. Leonard, H. M. van Driel, J. Schilling, and R. B. Wehrspohn, Phys. Rev. B **66**, 161102(R) (2002).
- [21] J. Manzanares-Martínez, F. Ramos-Mendieta, and P. Halevi, Phys. Rev. B **72**, 035336 (2005).
- [22] C. A. Barrios, V. R. Almeida, and M. Lipson, J. Lightwave Technol. **21**, 1089 (2003).
- [23] P. Dong, S. F. Preble, and M. Lipson, Opt. Express **15**, 9600 (2007).
- [24] K. Preston, P. Dong, B. Schmidt, and M. Lipson, Appl. Phys. Lett. **92**, 151104 (2008).
- [25] K. Busch and S. John, Phys. Rev. Lett. **83**, 967 (1999).
- [26] D. Kang, J. E. MacLennan, N. A. Clark, A. A. Zakhidov, and R. H. Baughman, Phys. Rev. Lett. **86**, 4052 (2001).
- [27] P. Halevi, J. A. Reyes-Avendaño, and J. A. Reyes-Cervantes, Phys. Rev. E **73**, 040701(R) (2006).
- [28] H. Kogelnik and C. V. Shank, Appl. Phys. Lett. **18**, 152 (1971).
- [29] H. Kogelnik and C. V. Shank, J. Appl. Phys. **43**, 2327 (1972).
- [30] N. Kroó, Zs. Szentirmay, and J. Féltszerfalvi, Phys. Lett. A **86**, 445 (1981).
- [31] D. Heitmann, N. Kroo, C. Schulz, and Z. Szentirmay, Phys. Rev. B **35**, 2660 (1987).
- [32] V. Celli, P. Tran, A. A. Maradudin, and D. L. Mills, Phys. Rev. B **37**, 9089 (1988).
- [33] P. Tran, V. Celli, and A. A. Maradudin, Opt. Lett. **13**, 530 (1988).
- [34] P. Halevi and O. Mata-Méndez, Phys. Rev. B **39**, 5694 (1989).